

Behavior of Buried Flexible Pipe under High Fills and Design Implications

Toshinori Kawabata¹; Hoe I. Ling²; Yoshiyuki Mohri, M.ASCE³; and Daisuke Shoda⁴

Abstract: The existing design guidelines for buried flexible pipes are limited to depth up to 10 m. The increasing use of difficult terrains for infrastructure, landfills, and residential and industrial developments has prompted installation of drainage pipelines under 20–30 m high fills. This paper presents the behavior of an instrumented flexible pipe buried under a 47.1 m deep fill. For filling above 20 m, the measured vertical stress above the pipe exhibited a concave distribution, corresponding to 90 and 110% of the average vertical pressure at the center and edges of the pipe, respectively. The measured results suggest that a triangular lateral pressure distribution can lead to overly conservative and uneconomical results for high fills while Spangler's analysis is unconservative. Based on the measured results, a revised vertical and lateral earth pressure diagram was proposed for the design of flexible pipe under high fills >20 m. This paper proposes closed-form analyses for estimating the moments and displacements of the pipe subjected to high fill earth pressures. These closed-form solutions agree well with the measured pipe displacements and strains.

DOI: 10.1061/(ASCE)1090-0241(2006)132:10(1354)

CE Database subject headings: Pipelines; Fills; Flexible pipes; Earth pressure; Deflection.

Introduction

The application of flexible pipes under high fills has not been very popular. Typically, irrigation and sewerage pipes of diameter exceeding 500 mm are limited to a cover depth of 10 m or less in Japan. Thus, recent installations of pipelines under high fills, such as landfill and residential and industrial sites have necessitated full-scale field instrumentation. The instrumentation on pipes under high fill is technically very difficult and costly, there are no previous data of this type published in the literature.

The analysis and design for the pipe buried under normal working stress conditions can be carried out using finite-element procedures (e.g., Katona et al. 1976). However, experimental results are always required to validate the numerical tools. Very limited field measurements are available for pipelines under high fills. Brown and co-workers (Brown 1967; Brown et al. 1968) examined the behavior of rigid and flexible culverts under 27 m

high fill, including comparing measurements and finite-element computations. Recently, Hashah and Selig (1990) and Meyer and Hilfiker (1996) reported on the study of a high-density polyethylene pipe of diameter 600 mm under a cover depth of 30 m.

In this paper, a pipe was monitored at a residential development site in Yamanashi Prefecture (Japan) during the period of construction of a fill 47.1 m high. A fiberglass reinforced plastic mortar (FRPM) pipe was used. The earth pressures, deflections, and strains in the pipe were measured over a period of 1 year. In addition, based on the field results, a comparison of two existing design procedures was conducted. A closed-form solution was obtained to determine the deflections and strains of the pipe corresponding to the measured behavior. The study led to a modified earth pressure diagram for high fill design.

Field Testing and Instrumentations

Fig. 1 shows the cross section of the instrumentation site in a valley where a 350 m long, 900 mm diameter pipe was installed inside a trench. The trench was prepared by excavating the ground up to 1.5 m. The water table was below this elevation. The pipe was a FRPM pipe with ring stiffness $EI=10.71$ kN m and wall thickness $t=18$ mm. The instrumented section was 4 m long. The mechanical properties of the FRPM pipe have been studied in detail by Kawabata (1993), the Young's modulus of FRPM, $E=22.05$ GPa.

A standard gravel (0–25 mm) was used as the backfill material around the pipe. Based on the compaction study conducted by Kawabata and Mohri (1995), the gravel was placed using 0.3 m lifts and each lift was compacted using two passes of 80 kg tamping rammer. The compacted gravel has a dry unit weight of 19.5–20.1 kN/m³. Its mean diameter and coefficient of uniformity were 6 mm and 27, respectively. The angle of internal friction obtained from triaxial compression tests under a confining pressure between 120 and 240 kPa was 52°. The stress–strain relationships for the gravels are given in Kawabata and Mohri

¹Associate Professor, Dept. of Agricultural and Environmental Engineering, Faculty of Agriculture, Kobe Univ., 1-1 Rokkodai, Nada, Kobe 657-8501, Japan. E-mail: Kawabata@kobe-u.ac.jp

²Associate Professor, Dept. of Civil Engineering and Engineering Mechanics, Columbia Univ., 500 West 120th St., New York, NY 10027, and Visiting Associate Professor, Division of Engineering and Applied Sciences, Harvard Univ. E-mail: ling@civil.columbia.edu

³Research Manager, Soil Mechanics Laboratory, National Institute for Rural Engineering, 2-1-6, Kannondai, Tsukuba, Ibaragi, Japan. E-mail: mohri@nkk.affrc.go.jp

⁴Graduate Student, School of Science and Technology, Kobe Univ., Japan. E-mail: 039d844n@y05.kobe-u.ac.jp

Note. Discussion open until March 1, 2007. Separate discussions must be submitted for individual papers. To extend the closing date by one month, a written request must be filed with the ASCE Managing Editor. The manuscript for this paper was submitted for review and possible publication on March 25, 2002; approved on May 6, 2006. This paper is part of the *Journal of Geotechnical and Geoenvironmental Engineering*, Vol. 132, No. 10, October 1, 2006. ©ASCE, ISSN 1090-0241/2006/10-1354–1359/\$25.00.

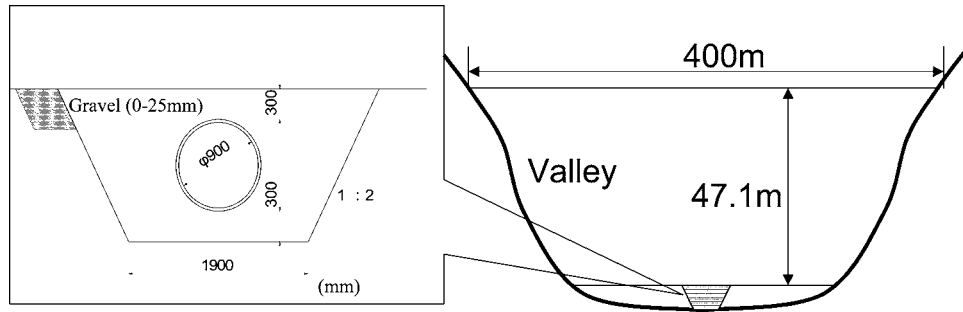


Fig. 1. Cross section of field test

(1995). The natural ground was a volcanic gravel tuff having a standard penetration resistance N value of 30–50. The fill above the pipe was a mixture of gravels and sands obtained from the field. No specific soil laboratory tests have been conducted on the natural soils or fills and all instrumentation was located on the pipe itself. The embankment construction took an additional year after the completion of filling around the pipe.

The field instrumentation consisted of three major quantities (Fig. 2): earth pressures, pipe deflections, and strains in the pipe, as described below:

- Three force transducers (100 mm diameter) were installed above the pipe at the center and edges to obtain the vertical stresses. Another transducer was installed at the spring line to measure the lateral earth pressure.
- Two linear variable differential transducers (LVDTs) were installed inside the pipe to measure its vertical and lateral deflections. The deflection across the pipe diameter was measured using a pulley-type LVDT such that the main body of the LVDT and the end of string were attached to the inner part of the pipe. In measuring for vertical displacement, a stand was hinged to the bottom of the pipe to which the LVDT was attached. Thus, the relative displacement between the two ends of the pipe was measured but not the absolute displacements of the two ends. For example, during filling, the crown and invert both moved downward, with the measured vertical deflection actually being the difference in these two movements.
- Strain gauges were installed on the outside of the pipe at a total of 12 locations. The circumferential strains of the pipe were thus obtained from the measurements. The strain gauges were glued to the pipe, followed by a layer of silicon, and finally protected by a layer of rubber sheet to be waterproof. The measurements were compensated for the effects of temperature using a dummy gauge.

The measurements were taken at 5.0 m height interval until the fill reached its final height of 47.1 m. A portable data logging

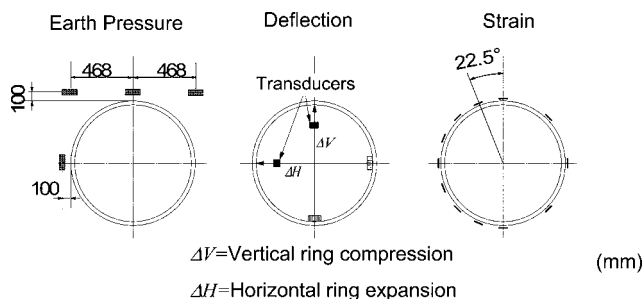


Fig. 2. Instrumentation of earth pressures, deflections, and strains

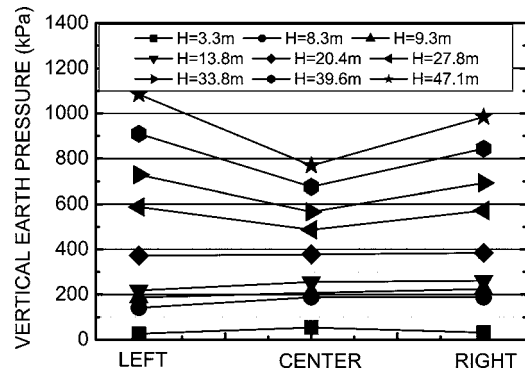
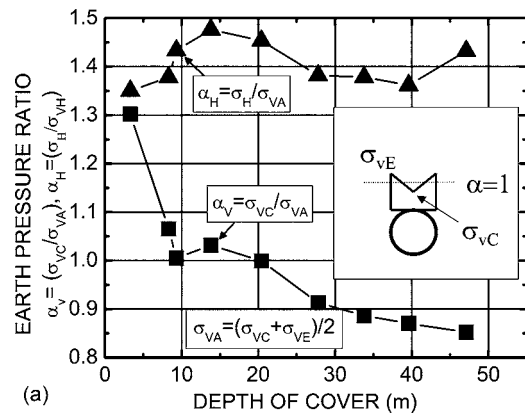
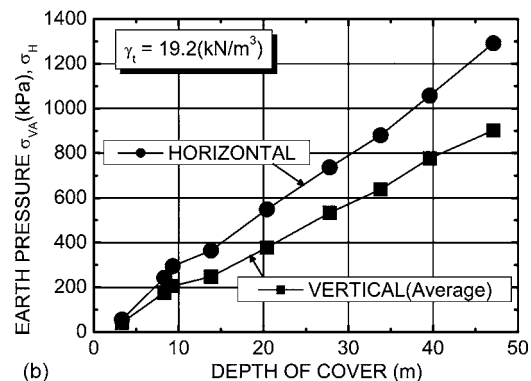


Fig. 3. Relationships between vertical stress distribution and cover depth



(a)



(b)

Fig. 4. Relationships between earth pressure ratios and cover depth

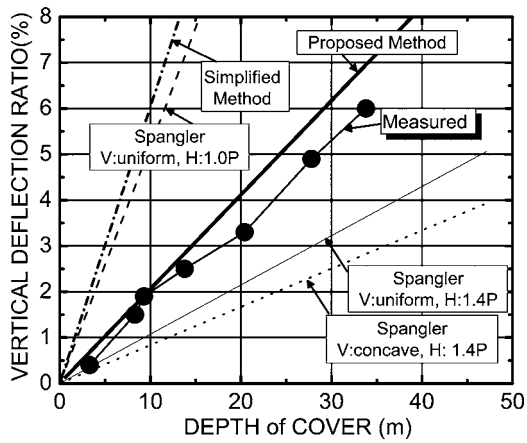


Fig. 5. Relationships between vertical deflection ratio and cover depth

system was used. The cables leading from the transducers to the ground surface were passed through a series of manholes, and the height was increased with construction.

Experimental Results

Earth Pressures

The variation of vertical earth pressures above the pipe under different fill heights is shown in Fig. 3. The distribution was approximately uniform up to a cover depth of 20 m, beyond which a concave shape was obtained. That is, the earth pressures at the edges were larger than those at the center of the upper portion of the pipe. For a cover depth of 47.1 m, the ratios of the pressure at the center (σ_{VC}) and edges (σ_{VE}) to the average vertical pressure (σ_{VA}) were 0.85 and 1.15, respectively, where $\sigma_{VA} = (\sigma_{VC} + \sigma_{VE})/2$. From 20 to 47.1 m, the ratios $\sigma_V = \sigma_{VC}/\sigma_{VA} = 0.9\sigma_{VE}/\sigma_{VA} = 1.1$. As shown in Fig. 4(a), α_V initially increased to 1.3 when the fill height was only 3 m to about 1.07 when the fill height was about 8 m. The initially larger value of vertical stress at the center compared to the ends was due to soil arching. The value of α_V thereafter generally decreased with increasing fill height, reaching 1.0 when the fill height was about

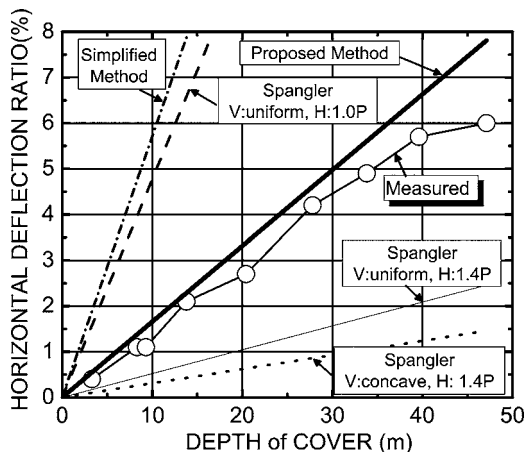


Fig. 6. Relationships between horizontal deflection ratio and cover depth

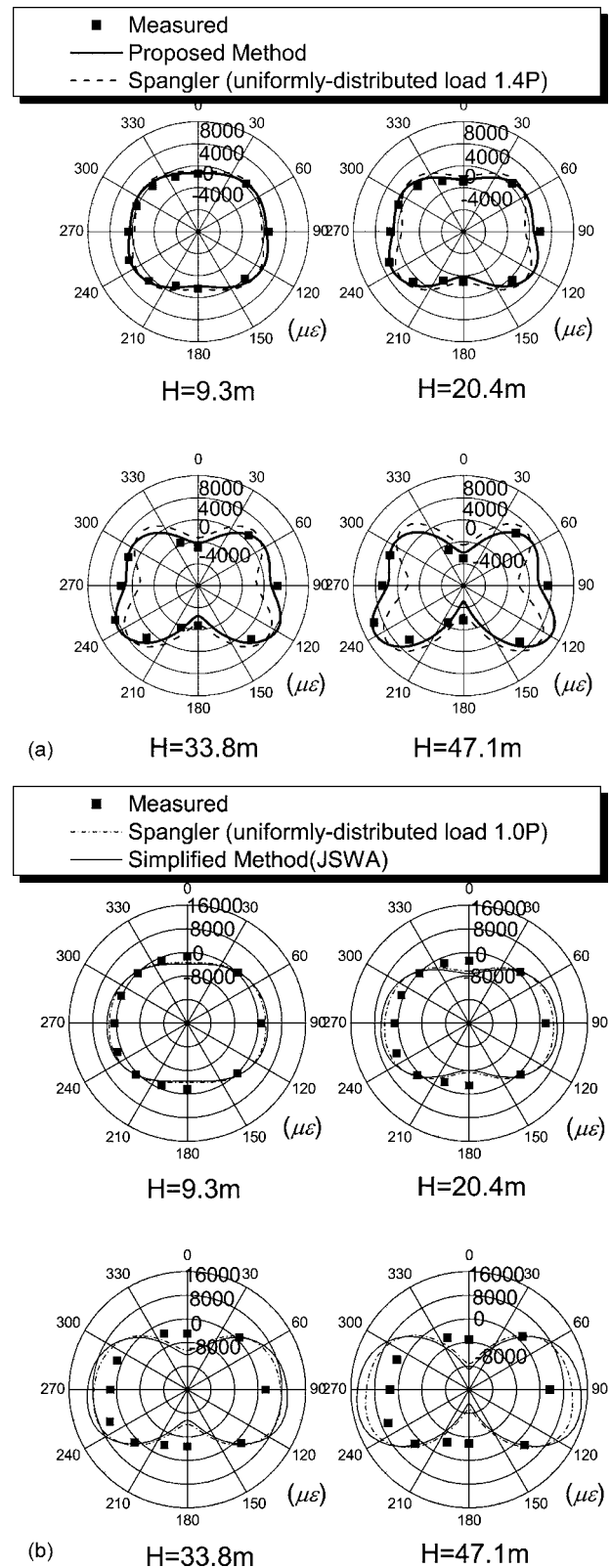


Fig. 7. Circumferential strains at different cover depths

20 m and about 0.85 when the fill height was 47 m. The concave vertical earth pressure distribution occurred when the pipe was subjected to high vertical loading that increased the deflections.

The unit weight of the fill, calculated from the averaged vertical stress, is shown in Fig. 4(b). The fill gave a rather constant unit weight of 19.2 kN/m³.

$$p = \sigma_{VA}$$

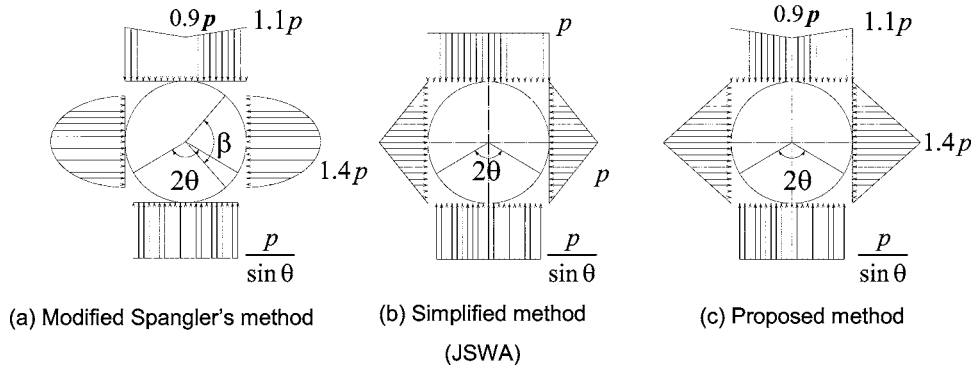


Fig. 8. Earth pressure diagram: (a) Spangler's analysis; (b) simplified analysis; and (c) proposed analysis

Similarly, α_H is defined as the ratio of the measured lateral earth pressure at the spring line α_H divided by the average measured vertical pressure, the ratio $\alpha_H \approx 1.4$ throughout construction [Fig. 4(a)].

Pipe Deflections

Figs. 5 and 6 show the relationship between the vertical and lateral deflection ratios of the pipe and fill height, respectively, where D = average of the inner and outer pipe diameters. Note that the vertical downward deflection (vertical ring compression) and horizontal outward deflection (horizontal ring expansion) were taken as positive. The measurement for the vertical ring compression stopped functioning after the fill reached a height of 33.8 m. The test results showed that the compaction of backfill material was good since a large horizontal reaction was obtained (Fig. 6) because the horizontal ring expansion was smaller than the vertical compression.

Circumferential Strains

The circumferential strains (tensile positive) of the outer surface of the pipe are shown in Fig. 7. At the final cover depth of 47.1 m, the largest compressive strain was measured at the top of the pipe ($-7071 \mu\epsilon$). On the other hand, the largest tensile strain

(5494 $\mu\epsilon$) was measured in the pipe at a location inclined at 22.5° below the spring line. The solid lines showing the calculated results will be discussed in the next section.

Earth Pressure Diagrams and Comparisons

For the analysis and design of flexible pipes, vertical and lateral earth pressure distributions have to be assumed. The method of Spangler (1941) is widely used for flexible pipe analysis and design, while a more simplified analysis is used typically for shallow buried water supply and sewerage pipe in Japan (JSWA 1999). The pressure diagrams for these analyses are shown in Fig. 8.

Spangler (1941) assumes a constant vertical stress $p = \sigma_{VA} = \gamma H$ and a parabolic lateral stress covering an angle of $\beta = 100^\circ$ [Fig. 8(a)]. The lateral pressure is essentially a function of the soil modulus of reaction. The lateral stress measured at the spring line, $\sigma_h = 1.4p$, is used in the calculation. The JSWA simplified analysis [Fig. 8(b)] assumes a constant vertical stress while the lateral pressure has a triangular distribution with a peak value equivalent to the vertical stress at the spring line, (i.e., $\sigma_h = p$).

The writers propose a third method based on the field measurements [Fig. 8(c)]. In this case the pipe has a nonuniform vertical earth pressure, with $0.9p$ at the center and $1.1p$ at the two edges. The lateral pressure distribution is triangular with a value of $1.4p$ at the spring line.

The bedding angle at the base, θ is a function of soil types and degree of compaction, among other factors. Based on the measured strain distribution, $\theta = 120^\circ$ was selected for gravels.

The elastic solution is derived for the assumed pressure diagrams in order to estimate the deflections and strains under high fills. The moment and axial force as well as the vertical and horizontal deflections due to the vertical and lateral earth pressures were determined separately and then superimposed, as illustrated in Fig. 9. The equations relating the moment and deflection calculations are summarized in Tables 1 and 2, respectively.

Figs. 5 and 6 show the comparisons between the computed and measured vertical ring compression and horizontal ring expansion. The proposed method resulted in linear relationships between fill height and deflections that deviated slightly from the measurements as fill height increased. It is seen that the vertical and horizontal deflections were determined quite satisfactorily.

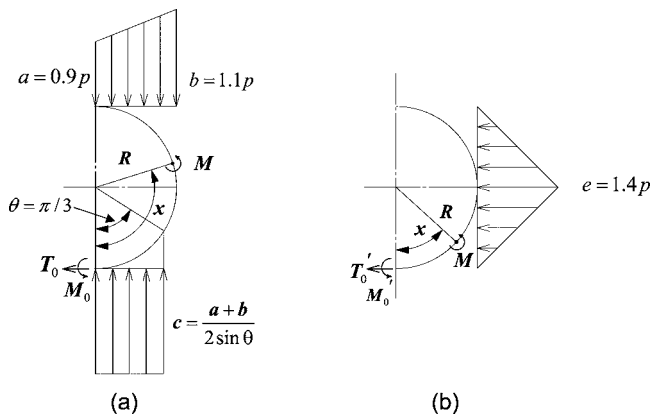


Fig. 9. Moments and axial force subject to (a) vertical earth pressure; (b) lateral earth pressure

Table 1. Moment Due to Vertical and Lateral Earth Pressures

Moment	Vertical earth pressure	Lateral earth pressure
$0 \leq x \leq \pi/3$	$M_1 = M_0 - T_0 \cdot R(1 - \cos x) - \frac{cR^2}{2} \sin^2 x$	$M_1 = M'_0 - T'_0 \cdot R \cdot (1 - \cos x)$
$\pi/3 \leq x \leq \pi/2$	$M_2 = M_0 - T_0 \cdot R(1 - \cos x) - cR^2 \left(\sin x \cdot \sin \theta - \frac{\sin^2 \theta}{2} \right)$	$-eR^2 \frac{1}{6} (-\cos^3 x + 3 \cos^2 x - 3 \cos x + 1)$
$\pi/2 \leq x \leq \pi$	$M_3 = M_0 - T_0 \cdot R(1 - \cos x) - cR^2 \left(\sin x \cdot \sin \theta - \frac{\sin^2 \theta}{2} \right)$ $-\frac{R^2}{6} \{3b(1 - \sin x)^2 - (b - a) \cdot (1 - \sin x)^3\}$	$M_2 = M'_0 - T'_0 \cdot R \cdot (1 - \cos x)$ $-eR^2 \frac{1}{6} (\cos^3 x + 3 \cos^2 x - 3 \cos x + 1)$
	$M_0 = \frac{R^2}{72\pi} \left\{ 12(a+b)\sin^2 \theta + 18(a+b)(\theta - \pi)\sin \theta + 27(a+b)\cos \theta \right.$ $\left. + 9(a+b)\frac{\theta}{\sin \theta} + 15\pi a + 12\pi b - 14a - 10b \right\}$	$M'_0 = e \cdot R^2 \left(-\frac{1}{12} - \frac{2}{9\pi} \right)$
	$T_0 = \frac{R}{12\pi} \{2(a+b)\sin^2 \theta - a - 3b\}$	$T'_0 = -\frac{eR}{2}$

On the other hand, the JSWA simplified method and Spangler's method with peak lateral pressure of p both overestimate the deflections. When a peak lateral pressure of $1.4p$ or a concave vertical pressure is assumed in Spangler's method, the deflections are underestimated (unconservative).

Fig. 7 compares the strains in the pipe obtained from several methods of analysis with field measurements at four different fill heights of 9.3, 20.4, 33.8, and 47.1 m. The measurements and solution obtained from the proposed analysis agreed very well throughout construction. However, for Spangler's analysis with a lateral peak pressure of $1.4p$ at the spring line, the results deviated from the measurements as the fill height increased [Fig. 7(a)]. It has to be noted that the difference between the measurements and Spangler's analysis was much larger when a peak value of p was assumed at the spring line [Fig. 7(b)]. The results obtained from the JSWA simplified method also deviated greatly from the measurements as the fill height increased. [Note that the scale of Fig. 7(b) is twice that of Fig. 7(a).]

Design Implications

The application of proposed earth pressure diagrams, moments, and deflections to design is illustrated in this section. For the proposed method [Fig. 8(c)], the maximum moment and maximum deflections are calculated using the equations of Tables 1 and 2, respectively, as a sum of contributions due to the vertical and lateral earth pressures:

- Maximum moment: $M_{\max} = 0.0573pR^2$;
- Maximum vertical deflection: $\Delta V_{\max} = -0.0238 \frac{pR^4}{EI}$; and
- Maximum horizontal deflection: $\Delta H_{\max} = 0.0192 \frac{pR^4}{EI}$.

Consider the geometry and properties of the FRPM pipe used in this study, the allowable stress of the pipe, $\sigma_{\text{allow}} = 314$ MPa. At the maximum backfill height of 47.1 m, $p = 902$ kPa, while $a = 828$ kPa, $b = 1,011$ kPa, $c = 1,287$ kPa according to Fig. 9. Hence, the computed maximum moment, $M_{\max} = 10.88$ kN m, while $\Delta V_{\max} = -88.8$ mm (-9.68%), and $\Delta H_{\max} = 71.6$ mm (7.8%).

Table 2. Deflections due to Vertical and Lateral Earth Pressures

Deflection	Vertical earth pressure	Lateral earth pressure
Vertical deflection $\Delta V = \Delta V_v + \Delta V_h$	$\Delta V_v = \frac{R^2}{EI} \left\{ 2M_0 - 2T_0 \cdot R - \frac{(a+b)R^2}{4 \sin \theta} \cdot \left(\frac{\cos^3 \theta}{3} - \cos \theta + \frac{2}{3} \right) \right.$ $\left. - \frac{(a+b)R^2}{2} \cdot \left(\frac{\pi}{2} - \frac{\sin \theta}{2} - \frac{\theta}{2} \right) - \frac{R^2}{6} \left(3a + 2b - \frac{15}{16}a\pi - \frac{9}{16}b\pi \right) \right\}$	$\Delta V_h = \frac{R^2}{EI} \left(2M'_0 - 2T'_0 R - \frac{7}{12} e \cdot R^2 \right)$
Horizontal deflection $\Delta H = \Delta H_v + \Delta H_h$	$\Delta H_v = \frac{2R^2}{EI} \left\{ M_0 - T_0 \cdot R \cdot \left(1 - \frac{\pi}{4} \right) \right.$ $\left. - \frac{(a+b)R^2}{12} (\sin^2 \theta - 3 \sin \theta + 3) \right\}$	$\Delta H_h = \frac{2R^2}{EI} \left\{ M'_0 - T'_0 \cdot R \cdot \left(1 - \frac{\pi}{4} \right) + e \cdot R^2 \cdot \left(\frac{5}{32} \pi - \frac{1}{2} \right) \right\}$

The largest stress developed in the pipe is $\sigma_{\max}=M_{\max}/Z$, where $Z=t^2/6$ is the section modulus. σ_{\max} is obtained as 202 MPa and corresponding strain $\epsilon_{\max}=\sigma_{\max}/E=9140 \mu\epsilon$. This maximum stress is less than the allowable value.

Summary and Conclusions

This paper presents measurements of earth pressures, deflections, and circumferential strains for a flexible pipe buried under high fill. The vertical earth pressure distribution was concave with the earth pressure at the center and edges of the pipe being 0.9 and 1.1 times that of the average vertical earth pressure, respectively. The lateral earth pressure at the spring line was 1.4 times the average vertical earth pressure across the top of the pipe.

These data were then used to propose a design diagram for flexible pipe buried under high fills and were used to compute the pipe deflections, strains, and bending moment.

Calculations of the pipe deflections and strains using the existing design earth pressure of Spangler (1941) and JSWA (1999) are not in good agreement with the measured data, while the proposed pressure diagrams and analysis gave very reasonable agreement with the measured results.

The results presented in this paper provided useful information in examining pipe behavior under high fills and for future validation of numerical and physical (such as centrifuge) modeling. The axial stress and buckling of the pipe under high fills are issues that warrant further study. Additional field instrumentation should

be conducted to further verify the proposed design procedures.

References

- Brown, C. B. (1967). "Forces on rigid culverts under high fills." *ASCE J. Struct. Div.*, 93(5), 195–215.
- Brown, C. B., Green, D. R., and Pawsey, S. (1968). "Flexible culverts under high fills." *ASCE J. Struct. Div.*, 94(4), 905–917.
- Hashah, N., and Selig, E. T. (1990). "Analysis of the performance of a buried high-density polyethylene pipe." *Structural performance of flexible pipes*, S. M. Sargand, G. F. Mitchell and J. O. Hurd, eds., Balkema, Rotterdam, The Netherlands, 95–103.
- Japanese Sewage Works Association (JSWA). (1999). *The design guidelines for fiberglass reinforced plastic mortar pipe*, JSWA, Tokyo.
- Katona, M. G., Smith, J. M., Odello, R. S., and Allgood, J. R. (1976). "CANDE—A modern approach for the structural design and analysis of buried culverts." *FHWA-RD-77-5*, Federal Highway Administration, Washington, D.C.
- Kawabata, T. (1993). "Mechanical behavior of buried flexible pipe." Ph.D. thesis, Kobe Univ., Kobe, Japan.
- Kawabata, T., and Mohri, Y. (1995). "Behavior of buried large thin wall flexible pipe—Field test and numerical analysis considered with stage of construction of buried flexible pipe." *Advances in underground pipeline engineering*, ASCE, Reston, Va., 13–24.
- Meyer, J. J., and Hilfiker, J. K. (1996). "High-density polyethylene pipe under high fill: A continuing study." *Pipeline crossings*, ASCE, Reston, Va., 77–81.
- Spangler, M. G. (1941). "The structural design of flexible pipe culverts," *Bulletin 153*, Iowa Engineering Experiment Station, Ames, Iowa.